JCIM JOURNAL OF CHEMICAL INFORMATION AND MODELING

pubs.acs.org/jcim

Application Note

FE-ToolKit: A Versatile Software Suite for Analysis of High-Dimensional Free Energy Surfaces and Alchemical Free Energy Networks

Timothy J. Giese, Ryan Snyder, Zeke Piskulich, German P. Barletta, Shi Zhang, Erika McCarthy, Şölen Ekesan, and Darrin M. York*

Cite This: *J. Chem. Inf. Model.* 2025, 65, 5273−5279

Read Online

ABSTRACT: Free energy simulations play a pivotal role in diverse biological applications, including enzyme design, drug discovery, and biomolecular engineering. The characterization of high-dimensional free energy surfaces underlying complex enzymatic mechanisms necessitates extensive sampling through umbrella sampling or string method simulations. Accurate ranking of target-binding free energies across large ligand libraries relies on comprehensive alchemical free energy calculations organized into thermodynamic networks. The predictive accuracy of these methods hinges on robust, scalable tools for networkwide data analysis and extraction of physical properties from heterogeneous simulation data. Here, we introduce `FE-ToolKit`, a versatile software suite for the automated analysis of free energy surfaces, minimum free energy paths, and alchemical free energy networks (thermodynamic graphs).

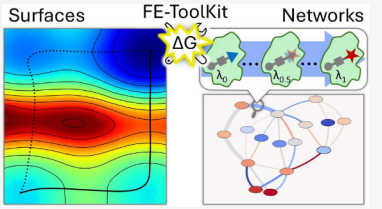

INTRODUCTION

The `FE-ToolKit` software is used to analyze and visualize high-dimensional free energy surfaces and alchemical free energy networks. `FE-ToolKit` consists of 3 main components: `ndfes`, `edgembar`, and `fetkutils`. The `ndfes` component analyzes umbrella sampling to produce multidimensional free energy surfaces[1] (FES) and optimize minimum free energy paths using the surface accelerated string method.[2] The `edgembar` component analyzes alchemical free energy (AFE) simulations[3] to calculate relative free energies between reference and target environments, e.g., in binding or solvation processes. The relative free energy simulations can be collected to form a topological network of transformations (sometimes referred to as a thermodynamic graph), and `edgembar` will perform networkwide free energy analysis to enforce cycle closure conditions and (optionally) additional experimental constraints.[4] The `fetkutils` component contains programs to choose optimized AFE λ-schedules.[5] Also contained in `fetkutils` are utilities to calculate kinetic isotope effects from umbrella sampling and path integral molecular dynamics (PIMD) simulations.[6] These tools have been described in detail elsewhere.[7]

Free energy applications analyze a large number of simulations. High-dimensional free energy surfaces often use data from many umbrella sampling simulations (sometimes several thousand[8]). AFE networks consist of multiple edges (transformations) composed of alchemical "λ states" simulated within several independent trials to obtain averages and error estimates. Specialized methods and algorithms are required to efficiently perform global FES[1] or networkwide AFE[4] analysis. In addition, one quickly becomes burdened with managing and examining hundreds (or thousands) of simulations to identify unequilibrated sampling, poor phase space overlap with neighboring states, data correlation, and statistical outliers. An automated process is necessary to detect problematic sampling and to summarize a wide array of potential issues for the user. The `FE-ToolKit` software includes algorithms for automatically detecting and discarding unequilibrated sampling. In addition, `FE-ToolKit` reports a wide array of indexes that can be used to alert the user to potential problems and analyses to facilitate troubleshooting. The details of these algorithms, a description of the error analysis, and an extended discussion of the theory are provided in the Supporting Information.

In summary, `FE-ToolKit` (Figure 1) provides the following features and capabilities:

- Multistate Bennett Acceptance Ratio[9] (MBAR) and/or variational free energy profile[1,10,11] (vFEP) analysis of high-dimensional free energy surfaces.
- Determination of minimum free energy paths using the surface accelerated string method.[2]
- Networkwide analysis of thermodynamic graphs with Lagrange multiplier constraints for cycle closure conditions and experimental priors.[4,12,13]

Received: March 12, 2025
Revised: May 8, 2025
Accepted: May 9, 2025
Published: May 21, 2025

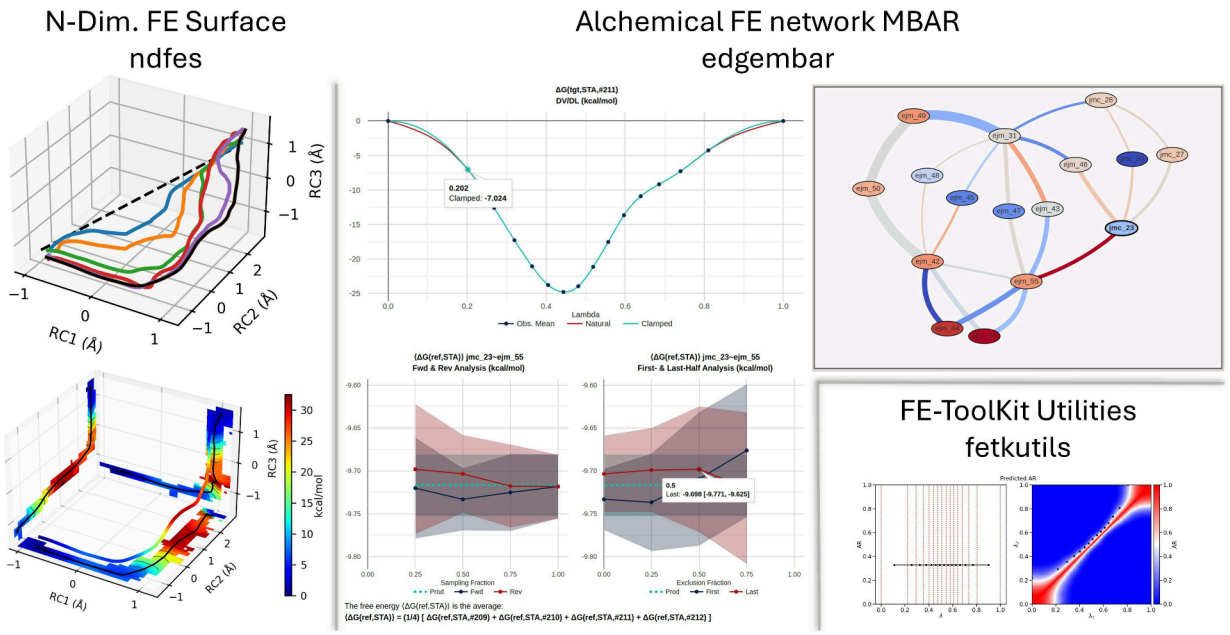

Figure 1. `FE-ToolKit` consists of `ndfes` for calculating *N*-dimensional free energy surfaces, `edgembar` for analyzing alchemical free energy networks using the EdgeMBAR method, and `FE-ToolKit` utilities (`fetkutils`) for optimizing schedules of alchemical states.

- Interoperability with equilibrium and nonequilibrium work simulations,[14−16] as well as indirect end state "book-ending" free energy corrections.[17]
- Automated determination of equilibrated sampling regions and outlier trial detection.
- Robust error analysis that considers correlation of time series data and independent trials, as well as cycle closure conditions.
- Trouble-shooting analysis, including calculation of Lagrange multiplier indexes, $dU/d\lambda$ profiles and variances, phase space overlap, and replica exchange efficiency.
- Tools for determination of optimized λ schedules using phase space overlap, Kullback−Leibler divergence and replica-exchange acceptance ratio methods.[5]

The Amber/AmberTools[18,19] software can perform GPU-accelerated alchemical free energy simulations with molecular mechanics force fields[12,13,20−22] and umbrella sampling simulations using generalized quantum mechanical/molecular mechanical and machine learning potentials.[23,24] This includes recently developed range-corrected deep-learning potentials,[25,26] graph neural network potentials,[27] and the QDπ models developed for drug discovery applications.[28,29] The `FE-ToolKit` package has been integrated into Amber-specific free energy workflows;[30] however, it reads data through its own input file formats rather than directly parsing simulation output. In this manner, the analysis programs are independent of the simulation package. The file formats are described here, the Supporting Information, and the Quick Start Tutorial.[31] The input, output, and command-line options of all software within `FE-ToolKit` use kcal/mol energy units unless explicitly overridden by the user.

UMBRELLA SAMPLING FREE ENERGY ANALYSIS

Umbrella sampling is used to study reaction mechanisms by introducing bias functions (harmonic potentials) to enhance the probability of observing rare configurations, such as transition states.[32−35] An unbiased FES is obtained with biased sampling performed along relevant reaction coordinate values using either the MBAR[9] or vFEP method.[4,10,11] Other analysis techniques include umbrella integration,[36−38] weighted histogram analysis[39,40] (WHAM), and unbinned WHAM[41,42] (UWHAM). The reweighting procedure can be extended to predict the FES of a target potential energy function from biased sampling obtained with inexpensive reference potentials. The weighted thermodynamic perturbation[43,44] (wTP) and generalized weighted thermodynamic perturbation[45] (gwTP) methods predict the high-level surface from sampling produced by one or more reference potentials, respectively.

The `ndfes` program produces multidimensional FESs by using the vFEP, MBAR, wTP, and gwTP methods. The input is a "metafile" whose lines describe the biased states. It is a generalization of the input used by Alan Grossfield's `WHAM` program.[46] Each state is characterized by an integer index ("Hamiltonian index") that denotes the unbiased potential energy function, the harmonic force constants and positions used during sampling, and the simulation temperature. Each line of the metafile also provides a "dumpave" filename whose rows are the observed samples and whose columns are the simulation time and the reaction coordinate values. Additional columns of unbiased potential energies of the reference and target potentials are included if a wTP or gwTP analysis is desired. The Hamiltonian index within the metafile indicates which of the extra columns corresponds to the sampled state's unbiased potential energy. The `ndfes` output is an Extensible Markup Language (XML) file that defines a multidimensional histogram and includes information for each occupied bin: the free energy value, standard error, the number of samples, and the reweighting entropy.[47] The `ndfes` input and output formats are independent of the molecular dynamics software used to generate the biased sampling; however, the `ndfes-PrepareAmberData.py` script is provided as a convenience to help create metafile and dumpave files from simulations performed with the sander software. Examples of

https://doi.org/10.1021/acs.jcim.5c00554
J. Chem. Inf. Model. 2025, 65, 5273−5279

the ndfes metafile and dumpave formats are found in the Supporting Information and Quick Start Tutorial.[31]

FE-ToolKit is packaged with utilities to prepare, analyze, and visualize FESs. The ndfes-CombineMetafiles.py script combines multiple metafiles to analyze aggregate sampling drawn from multiple trials. The ndfes-Avg-FESs.py script reads multiple FESs and outputs an average FES. The FE-ToolKit package includes examples that illustrate 2- and 3-dimensional FESs using the ndfes companion python library. The ndfes-CheckEquil.py utility uses the biasing potential time series to identify unequilibrated sampling within a dumpave file.

The ndfes-path program included within FE-ToolKit implements the surface-accelerate string method[2] (SASM) and the modified string method in collective variables.[48] The SASM method differs from other string methods[48−53] by propagating the string from the aggregate sampling produced from all previous iterations using fast methods for robust evaluation of high-dimensional free energy surfaces.[1] The available sampling is analyzed to produce a best estimate of the FES, and the current estimate of the minimum free energy path is optimized on the fixed surface.

The ndfes-genbias program is similar to ndfes; however, it does not assume that the simulations are biased with harmonic potentials. Instead, the values of the biasing potentials are read from extra columns within the dumpave files. The ndfes-genbias metafile format does not include umbrella window positions and force constants; it provides a "bias index" to indicate which of the extra columns corresponds to the bias used during sampling. Further details regarding the input format can be found in the Supporting Information. We recommend using ndfes rather than ndfes-genbias whenever possible. The ndfes input files and memory requirements are much smaller because it computes the bias potential as needed. The ndfes-genbias program is not yet capable of performing the vFEP method. Finally, one must exercise caution when aggregating the samples obtained from multiple trials and reference potentials because the "bias indexes" are invalidated if the metafiles do not use the same ordered set of biasing potentials. Similarly, all ndfes-genbias dumpave files would need to be completely rewritten if a new biasing potential was encountered.

■ ALCHEMICAL FREE ENERGY ANALYSIS

The edgembar program analyzes networks (graphs) of AFE simulations where the nodes and edges represent ligands and alchemical transformations, respectively. The free energy of an edge connecting ligands a and b is decomposed into contributions from two environments $\Delta\Delta G_{(ab)} = \Delta G_{(ab),\text{target}} - \Delta G_{(ab),\text{ref}}$. The transformation in an environment is decomposed into stages, $\Delta G_{(ab)e} = \sum_s \Delta G_{(ab)es}$, using either a one-stage softcore−electrostatic[54−56] or three-stage split protocol.[57] The free energy of a stage is an average of multiple independent simulation trials, $\Delta G_{(ab)es} = \langle \Delta G_{(ab)est} \rangle$, where t indexes the trial. A "trial" is a set of simulations performed at $N_{\text{state},(ab)est}$ states spanning $\lambda \in [0, 1]$, which define the potential energy, $U_{(ab)es}(\mathbf{r};\lambda)$. The trial's free energy is the difference between its final and initial states, $\Delta G_{(ab)est} = G_{(ab)est,\lambda=1} - G_{(ab)est,\lambda=0}$. MBAR analysis of trial t is equivalent to minimization of a convex objective function,[42] $F_{(ab)est}(\mathbf{G})$, with respect to $N_{\text{state},(ab)est}$ state free energies, $\mathbf{G}_{(ab)est}$.

$$F_{(ab)est}(\mathbf{G}_{(ab)est}) = \frac{1}{N_{s,(ab)est}} \sum_{j=1}^{N_{\text{state},(ab)est}} \sum_{k=1}^{N_{s,(ab)estj}} \times \ln\left(\sum_{l=1}^{N_{\text{state},(ab)est}} \exp[-\beta U_{(ab)es}(\mathbf{r}_{(ab)estjk};\, \lambda_l) - b_{(ab)estl}] \right) + \sum_{i=1}^{N_{\text{state},(ab)est}} \frac{N_{s,(ab)esti}}{N_{s,(ab)est}} b_{(ab)esti} \quad (1)$$

Here, $\beta = 1/k_B T$, where k_B is the Boltzmann's constant, T is the absolute temperature, $N_{s,(ab)esti}$ is the number of samples drawn from state i, $N_{s,(ab)est}$ is the aggregate number of samples within trial t, $\mathbf{r}_{(ab)estjk}$ is sample k in the ensemble of state j from trial t, and $b_{(ab)esti}$ is shown in eq 2.

$$b_{(ab)esti} = -\ln \frac{N_{s,(ab)esti}}{N_{s,(ab)est}} - \beta G_{(ab)esti} \quad (2)$$

Alternatively, one can define an objective function for the entire edge, $F_{(ab)}(\mathbf{G}_{(ab)})$, and simultaneously solve for every state in each environment, stage, and trial.

$$F_{(ab)}(\mathbf{G}_{(ab)}) = \sum_e \sum_{s=1}^{N_{\text{stage}}} \frac{\sum_{t=1}^{N_{\text{trial},(ab)es}} F_{(ab)est}(\mathbf{G}_{(ab)est})}{N_{\text{trial},(ab)es}} \quad (3)$$

The edge free energy is calculated from these values, $\Delta\Delta G_{(ab)}(\mathbf{G}^*_{(ab)})$, where the asterisk denotes the energies which minimize eq 3.

The sum of edge free energies along any closed path in the network should be zero; however, this is not guaranteed when the edges are independently analyzed. To rectify this, the MBARnet method[4] calculates every state in the network by minimizing a graph objective function (a sum of edge objectives) while imposing constraints to enforce closure conditions on minimal length cycles (cycles that cannot be formed by the union of smaller cycles). The MBARnet method has several shortcomings. The graph objective is expensive to evaluate; it requires a large amount of computer memory; the optimization needs to be performed if any new data or edges are added or removed; and enforcement of minimal length cycle closures does not guarantee that larger cycles will close.

The EdgeMBAR method avoids these shortcomings by introducing a graph objective function expressed in terms of $N_{\text{lig}} - 1$ ligand free energies. One ligand defines the arbitrary zero of energy, and the remaining free energies are relative to the reference $c_a = \Delta G_a - \Delta G_0$. The graph objective function is a sum of effective edge objectives $F(\mathbf{c}) = \sum_{(ab)} \tilde{F}_{(ab)}(c_b - c_a)$. The argument of an effective edge objective is a scalar value: the edge free energy. Values of the edge objective function can be pretabulated from constrained optimizations.

$$\tilde{F}_{(ab)}(x) = \min_{\mathbf{G}_{(ab)}} F_{(ab)}(\mathbf{G}_{(ab)}) \quad \text{subject to: } \Delta\Delta G_{(ab)}(\mathbf{G}_{(ab)}) = x \quad (4)$$

We observe that $F_{(ab)}(x)$ is well-modeled by a quadratic function centered about the unconstrained free energy, $g_{(ab)} = \Delta\Delta G^*_{(ab)}$, and whose force constant is fit to 5 points $x = \Delta\Delta G^*_{(ab)} \pm \delta$, where δ is 0, 1, or 2 kcal/mol. The graph objective and its solution for the ligand free energies are shown in eqs 5 and 6, respectively.

$$F(\mathbf{c}) = \sum_{(ab)} \frac{k_{(ab)}}{2} (c_b - c_a - g_{(ab)})^2 \quad (5)$$

https://doi.org/10.1021/acs.jcim.5c00554
J. Chem. Inf. Model. 2025, 65, 5273−5279

$$\mathbf{c} = \mathbf{M}^{-1}\cdot\mathbf{X}^{T}\cdot\mathbf{K}\cdot\mathbf{g} \quad (6)$$

$\mathbf{g}$ is a $N_{\text{edge}} \times 1$ array of unconstrained relative free energies, $\mathbf{K}$ is a $N_{\text{edge}} \times N_{\text{edge}}$ diagonal matrix of force constants, $K_{(ab),(cd)} = \delta_{(ab),(cd)}k_{(ab)}$, $\mathbf{X}$ is a $N_{\text{edge}} \times (N_{\text{lig}} - 1)$ matrix, $X_{(ab),c} = \delta_{bc} - \delta_{ac}$, and $\mathbf{M} = \mathbf{X}^{T}\cdot\mathbf{K}\cdot\mathbf{X}$. One may have accurate reference (experimental) values for a subset of the edges. These can be incorporated as linear constraints, as described in the Supporting Information.

The `edgembar` program analyzes simulation data for a single edge. It computes the state free energies and pretabulates the effective edge objective function (eq 4). The input is a XML file which organizes the simulation data into the hierarchy of environments, stages, trials, and states. The data from a trial are a collection of files named: "efep_*tlam*_*elam*.dat", where *tlam* is the sampled state, and *elam* is the state whose potential energies are tabulated within the file. The first column is the simulation time (ps), and the second column is a potential energy (kcal/mol). Further discussion and examples can be found in the Supporting Information and Quick Start Tutorial.[31] The `edgembar` output is organized into a data structure and written to a python file that can be imported directly into other scripts for analysis. Execution of the python output causes its results to be summarized in a HTML-formatted "edge report".

The `edgembar-WriteGraphHtml.py` script reads multiple `edgembar` outputs, calculates the ligand free energies (eq 6), and summarizes the results in a HTML-formatted "graph report", which compares the isolated edge free energies to the ligand free energy differences. Tables of closed paths and their closure errors are included. The graph and edge reports display energies in kcal/mol; however, future releases of `edgembar` will allow one to choose the output energy units. Reanalysis of the ligand free energies is inexpensive when new data is introduced because only the new edges need to be recalculated; the cost of solving the ligand free energies from eq 6 is small.

There are several existing python-based MBAR implementations for calculating state free energies in a trial.[58−60] `edgembar` is a C++ implementation that supports OpenMP parallelization but lacks GPU acceleration. The key feature of `edgembar` is its ability to simultaneously solve for all trials, stages, and environments while imposing constraints on the resulting $\Delta\Delta G$ to precalculate edge objective functions for networkwide analysis.

ALCHEMICAL λ SCHEDULES

The `fetkutils` component supplies the `fetkutils-tischedule.py` script for preparing application-specific AFE λ-schedules[5] to improve phase space overlap and the efficiency of Hamiltonian replica exchange (HRE). The MBAR method requires phase space overlap between states to produce reliable results.[9] Furthermore, poor overlap between any pair of adjacent states produces an exchange bottleneck in HRE simulations that adversely effect round-trip statistics.[61,62]

For a given number of states, the goal is to choose the simulated λ values to achieve uniform exchange rates or phase space overlap along the λ coordinate. To do this, one simulates an alchemical transformation for a brief amount of time with a large number of alchemical states (for example, 21 states) to ensure good phase space overlap between adjacent states. One then chooses a schedule size for production, and the scheduling script analyzes the "burn-in" simulations to optimize the λ values to minimize the variance in a property along the alchemical dimension (either the predicted replica exchange probability ratios, phase space overlap, or Kullback−Leibler divergence). An extensive discussion of the underlying theory is found in ref 5 and the Supporting Information. In addition to choosing the schedule size and property, one can also place conditions on the optimized schedule, such as enforcing symmetry about $\lambda = 0.5$.

CONCLUSIONS AND OUTLOOK

As free energy simulation methods advance to tackle increasingly complex problems, there is great need to develop robust, automated, efficient, and scalable analysis methods able to keep pace. These tools are critical to inform users of potential issues and provide data analytics needed to troubleshoot. `FE-ToolKit` was created to address these challenges and will continue to be developed and maintained to support emerging integrated free energy methods.

ASSOCIATED CONTENT

Data Availability Statement

`FE-ToolKit` software, full documentation, and a quick start guide are distributed under the MIT License at https://gitlab.com/RutgersLBSR/fe-toolkit or as part of the AmberTools package available at https://ambermd.org/AmberTools.php.

Supporting Information

The Supporting Information is available free of charge at https://pubs.acs.org/doi/10.1021/acs.jcim.5c00554.

A detailed discussion of the theory, algorithms, error analysis, file formats, and examples (PDF)

AUTHOR INFORMATION

Corresponding Author

Darrin M. York − *Laboratory for Biomolecular Simulation Research, Institute for Quantitative Biomedicine and Department of Chemistry and Chemical Biology, Rutgers University, Piscataway, New Jersey 08854, United States;* orcid.org/0000-0002-9193-7055; Email: Darrin.York@rutgers.edu

Authors

Timothy J. Giese − *Laboratory for Biomolecular Simulation Research, Institute for Quantitative Biomedicine and Department of Chemistry and Chemical Biology, Rutgers University, Piscataway, New Jersey 08854, United States;* orcid.org/0000-0002-0653-9168

Ryan Snyder − *Laboratory for Biomolecular Simulation Research, Institute for Quantitative Biomedicine and Department of Chemistry and Chemical Biology, Rutgers University, Piscataway, New Jersey 08854, United States*

Zeke Piskulich − *Laboratory for Biomolecular Simulation Research, Institute for Quantitative Biomedicine and Department of Chemistry and Chemical Biology, Rutgers University, Piscataway, New Jersey 08854, United States;* orcid.org/0000-0003-0304-305X

German P. Barletta − *Laboratory for Biomolecular Simulation Research, Institute for Quantitative Biomedicine and Department of Chemistry and Chemical Biology, Rutgers University, Piscataway, New Jersey 08854, United States;* orcid.org/0000-0002-0806-0812

Shi Zhang − *Laboratory for Biomolecular Simulation Research, Institute for Quantitative Biomedicine and*

https://doi.org/10.1021/acs.jcim.5c00554
J. Chem. Inf. Model. 2025, 65, 5273−5279

Department of Chemistry and Chemical Biology, Rutgers University, Piscataway, New Jersey 08854, United States; orcid.org/0000-0002-0281-9314

Erika McCarthy − *Laboratory for Biomolecular Simulation Research, Institute for Quantitative Biomedicine and Department of Chemistry and Chemical Biology, Rutgers University, Piscataway, New Jersey 08854, United States;* orcid.org/0000-0001-8089-0207

Şölen Ekesan − *Laboratory for Biomolecular Simulation Research, Institute for Quantitative Biomedicine and Department of Chemistry and Chemical Biology, Rutgers University, Piscataway, New Jersey 08854, United States;* orcid.org/0000-0002-5598-5754

Complete contact information is available at: https://pubs.acs.org/10.1021/acs.jcim.5c00554

Author Contributions

T.G. wrote the software and the manuscript. R.S., Z.P., P.B., S.Z, E.M., and S.E. reviewed the software and the manuscript. D.Y. directed the research.

Notes

The authors declare no competing financial interest.

■ ACKNOWLEDGMENTS

The authors are grateful for the financial support provided by the National Institutes of Health (Nos. GM62248 and GM107485) and the National Science Foundation (CSSI Frameworks Grant No. 2209718). Computational resources were provided by the Office of Advanced Research Computing (OARC) at Rutgers, The State University of New Jersey; the Advanced Cyberinfrastructure Coordination Ecosystem: Services & Support (ACCESS) program, which is supported by the National Science Foundation grants #2138259, #2138286, #2138307, #2137603, and #2138296 (supercomputer Expanse at SDSC through allocation CHE190067); the Texas Advanced Computing Center (TACC) at the University of Texas at Austin, URL: http://www.tacc.utexas.edu (supercomputer Frontera through allocation CHE20002); and the INCITE program through the Argonne Leadership Computing Facility at Argonne National Laboratory, which is supported by the Office of Science of the U.S. DOE under Contract No. DE-AC02-06CH11357 (supercomputer Polaris through INCITE allocation 13127).

■ REFERENCES

(1) Giese, T. J.; Ekesan, Ş.; York, D. M. Extension of the Variational Free Energy Profile and Multistate Bennett Acceptance Ratio Methods for High-Dimensional Potential of Mean Force Profile Analysis. *J. Phys. Chem. A* **2021**, *125*, 4216−4232.

(2) Giese, T. J.; Ekesan, Ş.; McCarthy, E.; Tao, Y.; York, D. M. Surface-Accelerated String Method for Locating Minimum Free Energy Paths. *J. Chem. Theory Comput.* **2024**, *20*, 2058−2073.

(3) York, D. M. Modern Alchemical Free Energy Methods for Drug Discovery Explained. *ACS Phys. Chem. Au* **2023**, *3*, 478−491.

(4) Giese, T. J.; York, D. M. Variational Method for Networkwide Analysis of Relative Ligand Binding Free Energies with Loop Closure and Experimental Constraints. *J. Chem. Theory Comput.* **2021**, *17*, 1326−1336.

(5) Zhang, S.; Giese, T. J.; Lee, T.-S.; York, D. M. Alchemical Enhanced Sampling with Optimized Phase Space Overlap. *J. Chem. Theory Comput.* **2024**, *20*, 3935−3953.

(6) Giese, T. J.; Zeng, J.; Ekesan, Ş.; York, D. M. Combined QM/MM, Machine Learning Path Integral Approach to Compute Free Energy Profiles and Kinetic Isotope Effects in RNA Cleavage Reactions. *J. Chem. Theory Comput.* **2022**, *18*, 4304−4317.

(7) Giese, T. J.; York, D. M. Estimation of frequency factors for the calculation of kinetic isotope effects from classical and path integral free energy simulations. *J. Chem. Phys.* **2023**, *158*, 174105−174115.

(8) Radak, B. K.; Romanus, M.; Lee, T.-S.; Chen, H.; Huang, M.; Treikalis, A.; Balasubramanian, V.; Jha, S.; York, D. M. Characterization of the Three-Dimensional Free Energy Manifold for the Uracil Ribonucleoside from Asynchronous Replica Exchange Simulations. *J. Chem. Theory Comput.* **2015**, *11*, 373−377.

(9) Shirts, M. R.; Chodera, J. D. Statistically optimal analysis of samples from multiple equilibrium states. *J. Chem. Phys.* **2008**, *129*, 124105.

(10) Lee, T.-S.; Radak, B. K.; Pabis, A.; York, D. M. A new maximum likelihood approach for free energy profile construction from molecular simulations. *J. Chem. Theory Comput.* **2013**, *9*, 153−164.

(11) Lee, T.-S.; Radak, B. K.; Huang, M.; Wong, K.-Y.; York, D. M. Roadmaps through free energy landscapes calculated using the multidimensional vFEP approach. *J. Chem. Theory Comput.* **2014**, *10*, 24−34.

(12) Lee, T.-S.; Tsai, H.-C.; Ganguly, A.; Giese, T. J.; York, D. M. In *Robust, Efficient and Automated Methods for Accurate Prediction of Protein-Ligand Binding Affinities in AMBER Drug Discovery Boost*; ACS Symposium Series; Armacost, K. A., Thompson, D. C., Eds.; ACS, 2021; Vol. *1397*; pp 161−204.

(13) Lee, T.-S.; Allen, B. K.; Giese, T. J.; Guo, Z.; Li, P.; Lin, C.; McGee, T. D.; Pearlman, D. A.; Radak, B. K.; Tao, Y.; Tsai, H.-C.; Xu, H.; Sherman, W.; York, D. M. Alchemical Binding Free Energy Calculations in AMBER20: Advances and Best Practices for Drug Discovery. *J. Chem. Inf. Model.* **2020**, *60*, 5595−5623.

(14) Boresch, S.; Woodcock, H. L. Convergence of single-step free energy perturbation. *Mol. Phys.* **2017**, *115*, 1200−1213.

(15) Kearns, F. L.; Hudson, P. S.; Woodcock, H. L.; Boresch, S. Computing converged free energy differences between levels of theory via nonequilibrium work methods: Challenges and opportunities. *J. Comput. Chem.* **2017**, *38*, 1376−1388.

(16) Schöller, A.; Kearns, F.; Woodcock, H. L.; Boresch, S. Optimizing the Calculation of Free Energy Differences in Non-equilibrium Work SQM/MM Switching Simulations. *J. Phys. Chem. B* **2022**, *126*, 2798−2811.

(17) Giese, T. J.; York, D. M. Development of a Robust Indirect Approach for MM → QM Free Energy Calculations That Combines Force-Matched Reference Potential and Bennett's Acceptance Ratio Methods. *J. Chem. Theory Comput.* **2019**, *15*, 5543−5562.

(18) Case, D.; Aktulga, H.; Belfon, K.; Ben-Shalom, I.; Berryman, J.; Brozell, S.; Cerutti, D.; Cheatham, I. T. E.; Cisneros, G.; Cruzeiro, V.; Darden, T.; Forouzesh, N.; Ghazimirsaeed, M.; Giambasu, G.; Giese, T.; Gohlke, H.; Goetz, A.; Harris, J.; Huang, Z.; LeGrand, S.; Li, P.; Luchko, T.; Luo, R.; Madej, B.; Merz, J.; Merz, J. K. M.; Monard, G.; Nguyen, C.; Nguyen, H.; Omelyan, I.; Onufriev, A.; Pan, F.; Qi, R.; Roe, D.; Roitberg, A.; Sagui, C.; Simmerling, C.; Swails, J.; Walker, R.; Wang, J.; Wolf, R.; Wu, X.; Xiao, L.; York, D.; Kollman, P. *Amber Reference Manual*; University of California, San Francisco, 2024.

(19) Case, D. A.; Aktulga, H. M.; Belfon, K.; Cerutti, D. S.; Cisneros, G. A.; Cruzeiro, V. W. D.; Forouzesh, N.; Giese, T. J.; Götz, A. W.; Gohlke, H.; Izadi, S.; Kasavajhala, K.; Kaymak, M. C.; King, E.; Kurtzman, T.; Lee, T.-S.; Li, P.; Liu, J.; Luchko, T.; Luo, R.; Manathunga, M.; Machado, M. R.; Nguyen, H. M.; O'Hearn, K. A.; Onufriev, A. V.; Pan, F.; Pantano, S.; Qi, R.; Rahnamoun, A.; Risheh, A.; Schott-Verdugo, S.; Shajan, A.; Swails, J.; Wang, J.; Wei, H.; Wu, X.; Wu, Y.; Zhang, S.; Zhao, S.; Zhu, Q.; Cheatham, T. E., 3rd; Roe, D. R.; Roitberg, A.; Simmerling, C.; York, D. M.; Nagan, M. C.; Merz, K. M., Jr AmberTools. *J. Chem. Inf. Model.* **2023**, *63*, 6183−6191.

(20) Lee, T.-S.; Hu, Y.; Sherborne, B.; Guo, Z.; York, D. M. Toward Fast and Accurate Binding Affinity Prediction with pmemdGTI: An Efficient Implementation of GPU-Accelerated Thermodynamic Integration. *J. Chem. Theory Comput.* **2017**, *13*, 3077−3084.

(21) Lee, T.-S.; Cerutti, D. S.; Mermelstein, D.; Lin, C.; LeGrand, S.; Giese, T. J.; Roitberg, A.; Case, D. A.; Walker, R. C.; York, D. M.

GPU-Accelerated Molecular Dynamics and Free Energy Methods in Amber18: Performance Enhancements and New Features. *J. Chem. Inf. Model.* **2018**, *58*, 2043−2050.
(22) Giese, T. J.; York, D. M. A GPU-Accelerated Parameter Interpolation Thermodynamic Integration Free Energy Method. *J. Chem. Theory Comput.* **2018**, *14*, 1564−1582.
(23) Giese, T. J.; Zeng, J.; Lerew, L.; McCarthy, E.; Tao, Y.; Ekesan, Ş.; York, D. M. Software Infrastructure for Next-Generation QM/MM-ΔMLP Force Fields. *J. Phys. Chem. B* **2024**, *128*, 6257−6271.
(24) Tao, Y.; Giese, T. J.; Ekesan, Ş.; Zeng, J.; Aradi, B.; Hourahine, B.; Aktulga, H. M.; Götz, A. W.; Merz, K. M., Jr; York, D. M. Amber free energy tools: Interoperable software for free energy simulations using generalized quantum mechanical/molecular mechanical and machine learning potentials. *J. Chem. Phys.* **2024**, *160*, 224104.
(25) Zeng, J.; Giese, T. J.; Ekesan, Ş.; York, D. M. Development of Range-Corrected Deep Learning Potentials for Fast, Accurate Quantum Mechanical/Molecular Mechanical Simulations of Chemical Reactions in Solution. *J. Chem. Theory Comput.* **2021**, *17*, 6993−7009.
(26) Wilson, T. J.; McCarthy, E.; Ekesan, Ş.; Giese, T. J.; Li, N.-S.; Huang, L.; Piccirilli, J. A.; York, D. M.; Lilley, D. M. J. The Role of General Acid Catalysis in the Mechanism of an Alkyl Transferase Ribozyme. *ACS Catal.* **2024**, *14*, 15294−15305.
(27) Zeng, J.; Giese, T. J.; Zhang, D.; Wang, H.; York, D. M. DeePMD-GNN: A DeePMD-kit Plugin for External Graph Neural Network Potentials. *J. Chem. Inf. Model.* **2025**, *65*, 3154−3160.
(28) Zeng, J.; Tao, Y.; Giese, T. J.; York, D. M. QDπ: A Quantum Deep Potential Interaction Model for Drug Discovery. *J. Chem. Theory Comput.* **2023**, *19*, 1261−1275.
(29) Zeng, J.; Tao, Y.; Giese, T. J.; York, D. M. Modern semiempirical electronic structure methods and machine learning potentials for drug discovery: Conformers, tautomers, and protonation states. *J. Chem. Phys.* **2023**, *158*, 124110.
(30) Ganguly, A.; Tsai, H.-C.; Fernández-Pendás, M.; Lee, T.-S.; Giese, T. J.; York, D. M. AMBER Drug Discovery Boost Tools: Automated Workflow for Production Free-Energy Simulation Setup and Analysis (ProFESSA). *J. Chem. Inf. Model.* **2022**, *62*, 6069−6083.
(31) Giese, T. J.; York, D. M. FE-ToolKit Quick Start Tutorial [Online]. https://rutgerslbsr.gitlab.io/fe-toolkit/quickstart (accessed April 2025).
(32) Torrie, G. M.; Valleau, J. P. Monte Carlo free energy estimates using non-Boltzmann sampling: Application to the sub-critical Lennard-Jones fluid. *Chem. Phys. Lett.* **1974**, *28*, 578−581.
(33) Torrie, G. M.; Valleau, J. P. Nonphysical sampling distributions in Monte Carlo free-energy estimation: Umbrella sampling. *J. Comput. Phys.* **1977**, *23*, 187−199.
(34) McDonald, I. R.; Singer, K. Machine Calculation of Thermodynamic Properties of a Simple Fluid at Supercritical Temperatures. *J. Chem. Phys.* **1967**, *47*, 4766−4772.
(35) McDonald, I. R.; Singer, K. Examination of the Adequacy of the 12−6 Potential for Liquid Argon by Means of Monte Carlo Calculations. *J. Chem. Phys.* **1969**, *50*, 2308−2315.
(36) Kästner, J.; Thiel, W. Bridging the gap between thermodynamic integration and umbrella sampling provides a novel analysis method: "Umbrella integration". *J. Chem. Phys.* **2005**, *123*, 144104.
(37) Kästner, J.; Thiel, W. Analysis of the statistical error in umbrella sampling simulations by umbrella integration. *J. Chem. Phys.* **2006**, *124*, 234106.
(38) Kästner, J. Umbrella integration in two or more reaction coordinates. *J. Chem. Phys.* **2009**, *131*, No. 034109.
(39) Kumar, S.; Bouzida, D.; Swendsen, R. H.; Kollman, P. A.; Rosenberg, J. M. The weighted histogram analysis method for free-energy calculations on biomolecules. *I. The method. J. Comput. Chem.* **1992**, *13*, 1011−1021.
(40) Souaille, M.; Roux, B. Extension to the weighted histogram analysis method: Combining umbrella sampling with free energy calculations. *Comput. Phys. Commun.* **2001**, *135*, 40−57.
(41) Zhang, B. W.; Xia, J.; Tan, Z.; Levy, R. M. A Stochastic Solution to the Unbinned WHAM Equations. *J. Phys. Chem. Lett.* **2015**, *6*, 3834−3840.
(42) Tan, Z.; Gallicchio, E.; Lapelosa, M.; Levy, R. M. Theory of binless multi-state free energy estimation with applications to protein-ligand binding. *J. Chem. Phys.* **2012**, *136*, 144102.
(43) Li, P.; Jia, X.; Pan, X.; Shao, Y.; Mei, Y. Accelerated Computation of Free Energy Profile at ab Initio Quantum Mechanical/Molecular Mechanics Accuracy via a Semi-Empirical Reference Potential. I. Weighted Thermodynamics Perturbation. *J. Chem. Theory Comput.* **2018**, *14*, 5583−5596.
(44) Hu, W.; Li, P.; Wang, J.-N.; Xue, Y.; Mo, Y.; Zheng, J.; Pan, X.; Shao, Y.; Mei, Y. Accelerated Computation of Free Energy Profile at Ab Initio Quantum Mechanical/Molecular Mechanics Accuracy via a Semiempirical Reference Potential. 3. Gaussian Smoothing on Density-of-States. *J. Chem. Theory Comput.* **2020**, *16*, 6814−6822.
(45) Giese, T. J.; Zeng, J.; York, D. M. Multireference Generalization of the Weighted Thermodynamic Perturbation Method. *J. Phys. Chem. A* **2022**, *126*, 8519−8533.
(46) Grossfield, A. WHAM: the weighted histogram analysis method [Online], version 2.1.0. http://membrane.urmc.rochester.edu/wordpress/?page_id=126 (accessed April 2025).
(47) Wang, M.; Li, P.; Jia, X.; Liu, W.; Shao, Y.; Hu, W.; Zheng, J.; Brooks, B. R.; Mei, Y. Efficient Strategy for the Calculation of Solvation Free Energies in Water and Chloroform at the Quantum Mechanical/Molecular Mechanical Level. *J. Chem. Inf. Model.* **2017**, *57*, 2476−2489.
(48) Rosta, E.; Nowotny, M.; Yang, W.; Hummer, G. Catalytic Mechanism of RNA Backbone Cleavage by Ribonuclease H from Quantum Mechanics/Molecular mechanics simulations. *J. Am. Chem. Soc.* **2011**, *133*, 8934−8941.
(49) E, W.; Ren, W.; Vanden-Eijnden, E. String method for the study of rare events. *Phys. Rev. B* **2002**, *66*, No. 052301.
(50) E, W.; Ren, W.; Vanden-Eijnden, E. Simplified and improved string method for computing the minimum energy paths in barrier-crossing events. *J. Chem. Phys.* **2007**, *126*, 164103.
(51) Maragliano, L.; Fischer, A.; Vanden-Eijnden, E.; Ciccotti, G. String method in collective variables: minimum free energy paths and isocommittor surfaces. *J. Chem. Phys.* **2006**, *125*, No. 024106.
(52) Ovchinnikov, V.; Karplus, M.; Vanden-Eijnden, E. Free energy of conformational transition paths in biomolecules: The string method and its application to myosin VI. *J. Chem. Phys.* **2011**, *134*, No. 085103.
(53) Zinovjev, K.; Tuñón, I. Adaptive Finite Temperature String Method in Collective Variables. *J. Phys. Chem. A* **2017**, *121*, 9764−9772.
(54) Beutler, T. C.; Mark, A. E.; van Schaik, R. C.; Gerber, P. R.; van Gunsteren, W. F. Avoiding singularities and numerical instabilities in free energy calculations based on molecular simulations. *Chem. Phys. Lett.* **1994**, *222*, 529−539.
(55) Lee, T.-S.; Lin, Z.; Allen, B. K.; Lin, C.; Radak, B. K.; Tao, Y.; Tsai, H.-C.; Sherman, W.; York, D. M. Improved Alchemical Free Energy Calculations with Optimized Smoothstep Softcore Potentials. *J. Chem. Theory Comput.* **2020**, *16*, 5512−5525.
(56) Tsai, H.-C.; Lee, T.-S.; Ganguly, A.; Giese, T. J.; Ebert, M. C.; Labute, P.; Merz, K. M., Jr; York, D. M. AMBER Free Energy Tools: A New Framework for the Design of Optimized Alchemical Transformation Pathways. *J. Chem. Theory Comput.* **2023**, *19*, 640−658.
(57) Klimovich, P. V.; Shirts, M. R.; Mobley, D. L. Guidelines for the analysis of free energy calculations. *J. Comput.-Aided Mol. Des.* **2015**, *29*, 397−411.
(58) Ding, X.; Vilseck, J. Z.; Brooks, C. L., III Fast Solver for Large Scale Multistate Bennett Acceptance Ratio Equations. *J. Chem. Theory Comput.* **2019**, *15*, 799−802.
(59) Beauchamp, K. A.; Chodera, J. D.; Naden, L. N.; Shirts, M. R. pymbar [Online], version 4.0. https://github.com/choderalab/pymbar (accessed April 2025).

https://doi.org/10.1021/acs.jcim.5c00554
J. Chem. Inf. Model. 2025, 65, 5273−5279

(60) Macdonald, H. B. cinnabar [Online], version 0.4.1. https://github.com/OpenFreeEnergy/cinnabar (accessed April 2025).
(61) Sidler, D.; Cristòfol-Clough, M.; Riniker, S. Efficient Round-Trip Time Optimization for Replica-Exchange Enveloping Distribution Sampling (RE-EDS). *J. Chem. Theory Comput.* **2017**, *13*, 3020−3030.
(62) Roe, D. R.; Bergonzo, C.; Cheatham, T. E. Evaluation of enhanced sampling provided by accelerated molecular dynamics with Hamiltonian replica exchange methods. *J. Phys. Chem. B* **2014**, *118*, 3543−3552.

https://doi.org/10.1021/acs.jcim.5c00554
J. Chem. Inf. Model. 2025, 65, 5273−5279